First-Principles Prediction of Vacancy Order-Disorder and Intercalation Battery Voltages in Li_xCoO_2

C. Wolverton and Alex Zunger
National Renewable Energy Laboratory, Golden, Colorado 80401
(Received 5 January 1998)

We present a first-principles technique for predicting the ordered vacancy ground states, intercalation voltage profiles, and voltage-temperature phase diagrams of Li intercalation battery electrodes. Application to the Li_xCoO_2 system yields correctly the observed ordered vacancy phases. We further predict the existence of additional ordered phases, their thermodynamic stability ranges, and their intercalation voltages in Li_xCoO_2/Li battery cells. Our calculations provide insight into the remarkable electronic stability of this system with respect to Li removal: A rehybridization of the Co-O orbitals acts to restore charge to the Co site ("self-regulating response"), thereby minimizing the effect of the perturbation. [S0031-9007(98)06670-8]

PACS numbers: 64.70.Kb, 65.50.+m, 71.15.Ap, 85.80.Dg

In intercalation systems such as Li in graphite, hydrogen in metals, and alkali metals in transition-metal dichalcogenides [1], the "guest" atom occupies certain "host" sites preferentially at low temperatures while others remain empty. Because of this specificity of the interactions between the guest atoms and the intercalation lattice sites, a wide variety of intercalated structures can form, including "ordered vacancy compounds." Ordered vacancy compounds of intercalated Li atoms have been observed in several layered lithium–transition-metal dichalcogenides such as Li_xTiS_2 [2], Li_xTaS_2 [3], and Li_xCoO_2 [4]. Above a critical temperature, these long-range ordered structures undergo an order-disorder transition into a phase where the vacancies are distributed in a disordered fashion on the intercalation sites. Many of these intercalation systems are of interest as high-energy density battery electrodes [1–4]. Since vacancy ordering in these compounds affects the electrochemical voltage, understanding intercalation ordering is important for tailoring the material to specific electrochemical applications. In this paper, we present a first-principles theoretical approach for *predicting* the new and unexpected stable vacancy-ordered structures, intercalation voltage profiles, and ultimately the voltage-temperature phase diagram of Li intercalation in the battery material Li_xCoO_2. Remarkably, despite the fact that the Li electron is needed to complete the octet shell of $LiCoO_2$, this system is electrochemically stable over a wide range of Li compositions, and thus electron numbers. We explain this "defect tolerance" in terms of a self-regulating response of the Co-O hybridization to the charge-altering Li intercalation.

$LiCoO_2$ has a layered rock-salt-based structure with two interpenetrating close-packed fcc sublattices: one sublattice consists of oxygen anions, and the other consists of Li and Co cations on alternating (111) planes. Vacancy ordering occurs on the Li sublattice which forms close-packed (111) planes yielding a two-dimensional triangular lattice. These Li-vacancy intercalation planes are stacked along $\langle 111 \rangle$ in a rhombohedral fashion (*ABC*). To study the intercalation ordering in Li_xCoO_2 on this stacked triangular lattice, we use a three-stage procedure [5,6].

In the *first step* of our method, we have calculated total energies for various ordered vacancy compounds constructed by removing Li atoms from the $LiCoO_2$ structure and distributing the ensuing vacancies (denoted by $\Box$) in different ways. The total energies have been obtained using the first-principles full-potential linearized augmented plane wave (LAPW) [7] method within the local density approximation (LDA) with the exchange correlation of Ceperley and Alder as parametrized by Perdew and Zunger. A well converged basis set (energy cutoff of 25.5 Ry) and Brillouin-zone integrations with equivalent meshes between $4 \times 4 \times 4$ and $8 \times 8 \times 8$ $\mathbf{k}$ points were used. All total energies were optimized with respect to volume as well as all cell-internal and cell-external coordinates [8]. Vacancy ordering within an intercalation plane as well as "staged" compounds (different compositions on neighboring planes) were considered. The energies of these structures σ are calculated relative to the composition-weighted average of the end points:

$$\Delta H(\sigma) = E(\mathrm{Li}_x\mathrm{CoO}_2;\sigma) - [xE(\mathrm{LiCoO}_2) + (1-x)E(\Box\mathrm{CoO}_2)]. \quad (1)$$

We find that $\Delta H < 0$ for all structures considered, thus indicating an ordering tendency between Li and $\Box$.

The *second step* of our method involves mapping these formation energies $\{\Delta H(\sigma)\}$ onto a generalized Ising-like model with 2-, 3-, and 4-body interactions [9], using the real-space cluster expansion (CE) technique (see, e.g., Refs. [5] or [6]): The pseudospin variable S_i is given the value $+1(-1)$ if a Li($\Box$) atom is assigned to a site i in the stacked triangular lattice. Then, the energy of *any* of the $2^N \gg 16$ configurations σ of Li and $\Box$ units can be written as

$$\Delta H_{\mathrm{CE}}(\sigma) = \sum_f D_f J_f \overline{\Pi}_f(\sigma), \quad (2)$$

 0031-9007/98/81(3)/606(4)$15.00

where f is a figure composed of several lattice sites (pairs, triplets, etc.) [9], D_f is the number of figures per lattice site, J_f is the Ising-like interaction for the figure f, and $\overline{\Pi}_f$ is a function defined as a product over the figure f of the variables S_i, averaged over all symmetry equivalent figures of lattice sites. We determine the effective interactions $\{J_f\}$ for the intercalation ordering problem by fitting $\Delta H_{\mathrm{CE}}(\sigma)$ of N_σ structures to LDA total energies $\Delta H_{\mathrm{LDA}}(\sigma)$. The stability of the expansion was verified by removing structures from the fitting procedure and predicting their energies from the resulting expansion. The resulting CE is stable, has first-principles accuracy, and has predictive power to describe the energetics of any intercalation configuration in $\mathrm{Li}_x\mathrm{CoO}_2$, even configurations of 100 000 atoms or more.

The *third step* of our approach involves subjecting the cluster expansion [Eq. (2)] to Monte Carlo simulations to ascertain both zero-temperature quantities (such as a prediction of the lowest-energy ordered vacancy phases) and finite-temperature properties (e.g., voltage profiles, order-disorder transitions, and the phase diagram associated with vacancy ordering). We use both canonical (fixed composition) and grand canonical (fixed chemical potential) simulations. System sizes of 8^3–$32^3 = 512$–$32\,768$ sites were used with between 200–200 000 spin flips per site. For our zero-temperature study, we explored the lowest-energy structures among these 8^3–32^3 sites using a simulated annealing algorithm.

Predicted stable ordered vacancy compounds.—The lowest-energy stable ordered vacancy compounds predicted (out of the astronomical number of 2^N possible compounds) are shown in Fig. 1 as a function of Li content. Some of the predicted ground states are included in the original set of LDA-calculated energies (filled squares), but some are not (empty squares), and, hence, are truly unsuspected predictions. Our ground state calculations are in agreement with the observed ground state at $x = 1/2$: Reimers and Dahn [4] have observed electrochemically and through x-ray diffraction a monoclinic ordered vacancy compound at $x = 1/2$. Their data suggest a "2×1" two-dimensional ordering as we have predicted. The cluster expansion [Eq. (2)] also affords calculation of the energetics of configurations which are too complicated for direct LDA techniques, e.g., the energy of the random arrangement of Li and □ units as a function of composition (Fig. 1). Also, we note that the cluster expansion constructed here is for a substitutional problem on a fixed lattice type (triangular planes with *ABC* stacking). However, it has been observed [10] and subsequently confirmed via first-principles energetics [11] that a shuffling of lattice planes occurs for low-Li content where the structure transforms in a nonsubstitutional manner to an *AAA*-type of stacking. We consider here only substitutional arrangements of Li and □ for an *ABC* cation stacking, and, hence, do not account for possible vacancy ordered compounds which might occur on different lattice stackings (e.g., *AAA*) for low-Li content ($x \lesssim 1/3$).

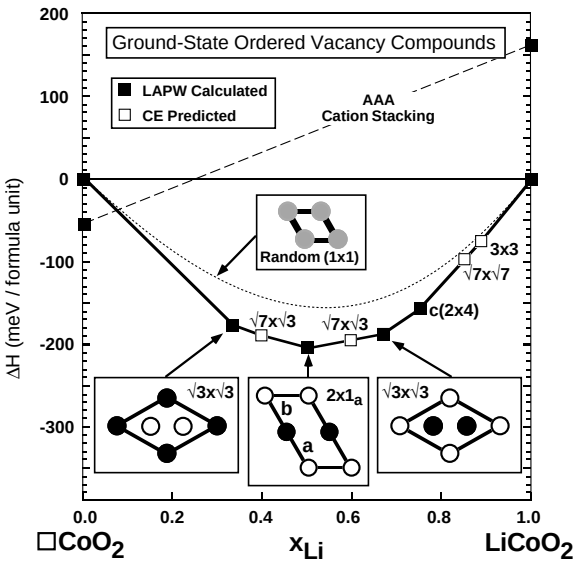

FIG. 1. Predicted ordered vacancy ground state structures of $\mathrm{Li}_x\mathrm{CoO}_2$. The filled squares are LAPW results, and the open squares are CE results. The random "alloy" with a random arrangement of Li and □ is shown as a dotted line. 2D representations (Li-vacancy ordering in a single close-packed Li plane) of some of the predicted 3D ordered vacancy compounds in $\mathrm{Li}_x\mathrm{CoO}_2$ are also shown (filled circles, Li; empty circles, vacancy). In the $x = 1/2$ phase ($2 \times 1_a$), there are two inequivalent positions where Li atoms may be placed in the neighboring planes (labeled "a" and "b"). We find the "$2 \times 1_a$" structure to be lower in energy than "$2 \times 1_b$".

Electronic stability with respect to Li removal.—$R\bar{3}m$-ordered stoichiometric LiCoO_2 is an insulator in LDA [12,13], but Li removal (Fig. 1) moves the Fermi level into the valence band, turning the system (in LDA) to a metal. The classic inorganic-chemistry view of this reaction is that the Co ion absorbs the charge change: it changes its oxidation state from Co^{3+} in LiCoO_2 to Co^{4+} in $\square\mathrm{CoO}_2$. Considering the large (Mott-Hubbard) Coulomb energy of an unhybridized transition metal ion [14], such a change in oxidation state would be accompanied by substantial modification of the energy level structure of LiCoO_2, which is not observed in our self-consistent calculations. Instead, we find that the charge enclosed around the Co site is surprisingly constant (7.36 ± 0.04 valence electrons inside a radius of 1.06 Å) for all configurations, as the Li content is reduced from $x = 1$ to $x = 0$ [15]. Figure 2 shows the charge rearrangements due to complete $[\rho(\mathrm{LiCoO}_2)$-$\rho(\square\mathrm{CoO}_2)]$ and partial $[\rho(\mathrm{LiCoO}_2)$-$\rho(\mathrm{Li}_{0.5}\mathrm{CoO}_2)]$ Li removal, assuming the same lattice parameters and atomic positions (those of relaxed LiCoO_2) for all structures. This figure demonstrates that as electronic charge is removed from the compound (via Li extraction), the oxygen-cobalt hybridization changes, so as to maintain a nearly constant charge (hence, nearly unchanged energy levels) around

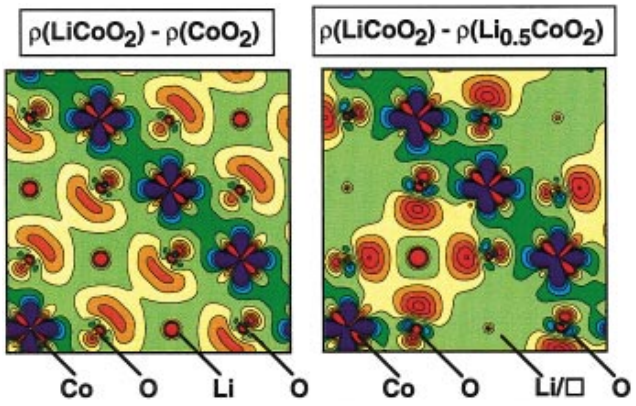

FIG. 2(color). Calculated charge density differences between $LiCoO_2$, $Li_{0.5}CoO_2$, and $\square CoO_2$ (all at the fixed, relaxed geometry of $LiCoO_2$) showing the change in Co-O hybridization upon Li removal (the self-regulating response). Red regions show the large positive charge density differences (charge density diminishes upon removal of Li) while blue regions indicate negative differences (charge density is enhanced upon Li removal).

the Co site. This "self-regulating response" [14,16] (minimizing the effect of external perturbations via rehybridization) is characteristic of systems having localized d states that communicate with a covalent manifold, e.g., transition-atom impurities in semiconductors [16]. It explains in such systems why the d-like energy levels do not shift significantly in response to large nominal changes in charge, and thus at least partly explains the defect tolerance of these structures over a large range of Li concentrations (Fig. 1).

First-principles prediction of Li_xCoO_2/Li voltage profile.—For a Li_xCoO_2/Li cell at temperature T, the voltage $V(x)$ as a function of Li composition is given by [1,17] the Li chemical potential difference between cathode (Li_xCoO_2) and anode (Li metal):

$$-eV(x,T) = \mu_{\mathrm{Li}}(\mathrm{Li}_x\mathrm{CoO}_2, T) - \mu_{\mathrm{Li}}(\mathrm{Li\ metal}, T)\,. \tag{3}$$

Using a static, bulk description, the chemical potential of Li metal is a constant reference energy and is independent of T. Thus, computing the voltage of Eq. (3) amounts to computing the chemical potential $\mu_{\mathrm{Li}}(\mathrm{Li}_x\mathrm{CoO}_2, T)$ relative to the reference of Li metal. This chemical potential as a function of Li content and temperature may be computed [17] up to a constant reference [18] from grand canonical (i.e., fixed chemical potential) Monte Carlo simulations of the Li_xCoO_2 cluster expansion at finite T. This provides a completely parameter-free, first-principles prediction of the Li intercalation voltage of the Li_xCoO_2/Li cell as a function of Li content.

The predicted intercalation voltage profiles are shown in Fig. 3. Two-phase regions, defined in terms of free energies vs x by tie lines connecting the two phases, correspond to plateaus in the voltage profiles. Likewise, the voltage drops are associated with single phase, ordered regions. As the temperature is increased, drops become more rounded and disappear at order-disorder transitions. The voltage profile of the solid solution phase is completely smooth with no discontinuous voltage drops. Measured voltage profiles (see, e.g., Refs. [4,10]) show an average voltage of around 4.0–4.2 V with a drop in voltage of ~0.6–0.8 V with composition, while our first-principles predictions show an average of 3.8 V with a ~1.3 V drop with composition. (Note that both this overall calculated voltage drop and the voltage drop associated with the $x = 1/3$ ordered phase are decreased by ~0.2 V if one includes the low energy of the *AAA*-stacked $\square CoO_2$ compound. However, all voltage calculations in Fig. 3 are for *ABC* stacking.) Also, we find no evidence for a two-phase region for Li-rich compositions, as reported from electrochemical measurements [4,10].

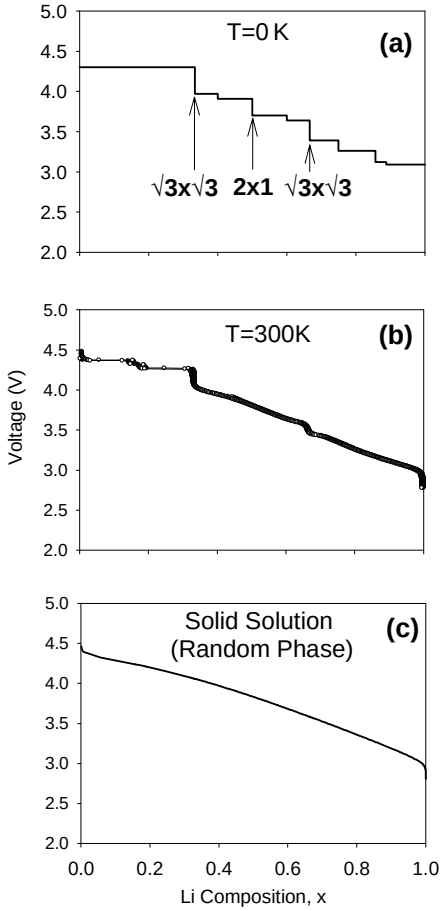

FIG. 3. Predicted Li-intercalation voltage of the Li_xCoO_2/Li cell as a function of Li composition, calculated from the chemical potential difference in Eq. (3). (a) Equilibrium profile at $T = 0$ K, calculated analytically from the slopes of the ground state hull in Fig. 1. (b) Equilibrium profile at $T = 300$ K, calculated from Monte Carlo simulations. (c) Profile of the metastable random solution phase, calculated analytically from the cluster expansion interactions with mean-field ($T = 300$ K) entropy.

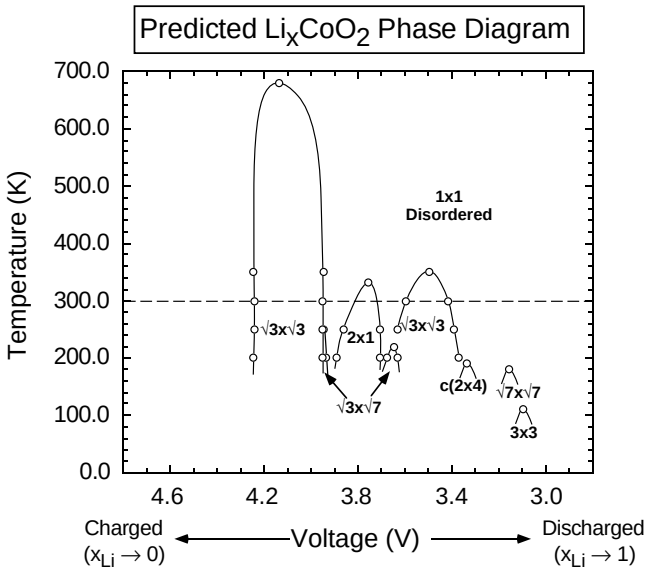

FIG. 4. Predicted Li_xCoO_2 voltage-temperature phase diagram. Note that at room temperature (horizontal dashed line), three vacancy compounds remain ordered. Also, for low enough Li content, the system undergoes a transition (not shown) to an *AAA* type of stacking. (Only *ABC* stackings are considered in the calculation of this phase diagram.)

Equilibrium Li-intercalation Li_xCoO_2 phase diagram.—Via a combination of Monte Carlo simulations (both grand canonical and canonical), thermodynamic integration, and investigation of finite-size effects, one can map the entire chemical potential-temperature (and, hence, the voltage-temperature) phase diagram for Li intercalation in Li_xCoO_2/Li cells. The predicted phase diagram is shown in Fig. 4. Many of the predicted ground state phases (Fig. 1) undergo order-disorder transitions below room temperature. In equilibrium, three phases are predicted to remain ordered at and above room temperature: the 2×1 ($x = 1/2$) and $\sqrt{3} \times \sqrt{3}$ ($x = 1/3$ and $2/3$) structures. The predicted stability range of the 2×1 ($x = 1/2$) phase is in good agreement with electrochemical observations: Reimers and Dahn [4] have measured the order-disorder transition temperature for this phase at 60 °C, and the width of the 2×1 phase field at room temperature to be $\sim$0.1 V. Our calculations are in excellent agreement with both of these observations. No compounds at $x = 1/3$ or $x = 2/3$ have been experimentally reported in Li_xCoO_2 (although these $\sqrt{3} \times \sqrt{3}$ phases have been found in other layered intercalation compounds). It is possible that the formation of these phases is kinetically inhibited in electrochemical experiments. Future electrochemical experiments to investigate the thermodynamic stability of the predicted ordered vacancy phases would therefore be of great interest.

Helpful discussions with David Ginley, Jeanne McGraw, Phil Parilla, and John Perkins are gratefully acknowledged. This work was supported by the Office of Energy Research (OER) [Division of Materials Science of the Office of Basic Energy Sciences (BES)], U.S. Department of Energy, under Contract No. DE-AC36-83CH10093.

[1] W. R. McKinnon and R. R. Haering, in *Modern Aspects of Electrochemistry,* edited by R. E. White, J. O'M. Backris, and B. E. Conway (Plenum, New York, 1983), Vol. 15, p. 235.
[2] A. H. Thompson, Phys. Rev. Lett. **40**, 1511 (1978).
[3] W. R. McKinnon and J. R. Dahn, Solid State Commun. **48**, 43 (1983).
[4] J. N. Reimers and J. R. Dahn, J. Electrochem. Soc. **139**, 2091 (1992).
[5] A. Zunger, in *Statics and Dynamics of Alloy Phase Transformations,* NATO ASI, Ser. B, Vol. 319 (Plenum Press, New York, 1994), p. 361.
[6] D. de Fontaine, Solid State Phys. **47**, 33 (1994).
[7] D. J. Singh, *Planewaves, Pseudopotentials, and the LAPW Method* (Kluwer, Boston, 1994).
[8] Many of the ordered vacancy compounds considered are of monoclinic (or lower) symmetry. In all cases the lengths of the unit-cell vectors were allowed to vary; however, the energetic effect of distorting the monoclinic angle from its ideal position was neglected.
[9] In fitting the expansion of Eq. (2), we have used total energies for 16 ordered vacancy compounds and the following 12 figures (and the corresponding interactions): empty, point, first- through fifth-neighbor "in-plane" pairs (connecting sites in a single triangular plane), two in-plane triplets, one in-plane quadruplet, and two "out-of-plane" pairs (connecting two neighboring triangular planes).
[10] G. G. Amatucci, J. M. Tarascon, and L. C. Klein, J. Electrochem. Soc. **143**, 1114 (1996).
[11] C. Wolverton and A. Zunger, Phys. Rev. B **57**, 2242 (1998).
[12] M. T. Czyzyk, R. Potze, and G. A. Sawatzky, Phys. Rev. B **46**, 3729 (1992).
[13] M. K. Aydinol, A. F. Kohan, G. Ceder, K. Cho, and J. Joannopoulos, Phys. Rev. B **56**, 1354 (1997).
[14] A. Zunger, Solid State Phys. **39**, 275 (1986).
[15] Although the qualitative charge densities are similar to the present results, a larger variation in Co charge was found by Aydinol *et al.* [13] who used pseudopotential calculations (rather than the present all-electron calculations) and found a change of 0.28 electrons on the Co site (radius of 0.98 Å) upon delithiation. We find a change of 0.04 electrons (radius of 1.06 Å).
[16] F. D. M. Haldane and P. W. Anderson, Phys. Rev. B **13**, 2553 (1976).
[17] J. N. Reimers and J. R. Dahn, Phys. Rev. B **47**, 2995 (1993).
[18] The reference energy of Eq. (1) is not that of pure Li metal. Thus, to obtain the correct reference energy for the intercalation voltage of Eq. (3), we must add the linear function of composition (constant chemical potential), $x\overline{V} = x[E(\mathrm{Li}_x\mathrm{CoO}_2)\text{-}E(\square\mathrm{CoO}_2)\text{-}E(\mathrm{Li\ metal})]$, to Eq. (1). The "average voltage" $\overline{V}$ (i.e., the voltage integrated over Li composition [13]) has been computed to be 3.78 V from LAPW total energies [11].